Functional Characterization of the Bacterial *iac* Genes for Degradation of the Plant Hormone Indole-3-Acetic Acid

Jeness C. Scott · Isaac V. Greenhut · Johan H. J. Leveau

Abstract *Pseudomonas putida* 1290 is a model organism for the study of bacterial degradation of the plant hormone indole-3-acetic acid (IAA). This property is encoded by the *iac* gene cluster. Insertional inactivation and/or deletion of individual *iac* genes and heterologous expression of the gene cluster in *Escherichia coli* were combined with mass spectrometry to demonstrate that *iac*-based degradation of IAA is likely to involve 2-hydroxy-IAA, 3-hydroxy-2-oxo-IAA, and catechol as intermediates. The first gene of the cluster, *iacA* encodes for the first step in the pathway, and also can convert indole to indoxyl to produce the blue pigment indigo. Transcriptional profiling of *iac* genes in *P. putida* 1290 revealed that they were induced in the presence of IAA. Based on results with an *iacR* knockout, we propose that this gene codes for a repressor of *iacA* expression and that exposure to IAA relieves this repression. Transformation of *P. putida* KT2440 (which cannot degrade IAA) with the *iac* gene cluster conferred the ability to grow on IAA as a sole source of carbon and energy, but not the ability to chemotaxi towards IAA. We could show such tactic response for *P. putida* 1290, thus representing the first demonstration of bacterial chemotaxis towards IAA. We discuss the ecological significance of our findings, and specifically the following question: under what circumstances do bacteria with the ability to degrade, recognize, and move towards IAA have a selective advantage?

Keywords Auxin · Indigo · Chemotaxis · *Pseudomonas putida*

Introduction

The ability of bacteria to destroy chemicals with hormonal activity in higher organisms has been well documented (Dodd *et al.* 2010; Garcia-Gomez *et al.* 2013). In plants, indole-3-acetic acid (IAA) is an auxin hormone that plays a key role in plant growth and development (Gray 2004). Bacteria from various environments can inactivate or even mineralize IAA (Faure *et al.* 2009; Leveau and Gerards 2008; Leveau and Lindow 2005). The ecological function of this activity remains unknown. Does it provide bacteria with a selective advantage in habitats that feature IAA in quantities sufficiently large to serve as an alternative source of carbon, nitrogen, and/or energy? Or does it allow bacteria to alter plant IAA homeostasis and indirectly manipulate plant physiology in a way that confers some as-of-yet-unknown gain in bacterial survival or reproduction? Knowing that plants are not the only source of IAA (Patten and Glick 1996), and that IAA may act as a signal molecule between microorganisms (Spaepen *et al.* 2007) evokes even more questions about the possible role and ecological significance of bacterial IAA degradation. Answering such questions will require a more complete understanding of the genes and gene products that are involved in this activity.

Our lab has used the bacterial isolate *Pseudomonas putida* 1290 as a model strain for the identification and characterization of IAA-degradative genes. This bacterium originally was isolated from pear tree foliage and it efficiently exploits IAA as a nutrient source (Leveau and Lindow 2005). Taking a forward genetics approach (Leveau and Gerards 2008), it

J. C. Scott · I. V. Greenhut · J. H. J. Leveau (✉)
Department of Plant Pathology, University of California, One Shields Avenue, Davis, CA 95616, USA
e-mail: jleveau@ucdavis.edu

Present Address:
J. C. Scott
Department of Plant Pathology, University of Minnesota, Minneapolis, MN 55108, USA

was discovered that IAA mineralization by *P. putida* 1290 involved an 8,994-bp genomic DNA fragment that when transferred to *P. putida* KT2440 rendered this strain able to grow on IAA (Leveau and Gerards 2008). Homologs of the ten so-called *iac* genes on this DNA fragment were identified in clusters on the genomes of various representatives from the α-, β-, and γ-Proteobacteria, as well as high G+C Gram-positive bacteria (Leveau and Gerards 2008), and the ability to grow on IAA was confirmed for several of these bacterial strains (Leveau and Gerards 2008), including most recently the strain *Acinetobacter baumannii* ATCC 19606 (Lin *et al.* 2012).

Little is known still about the contribution of individual *iac* genes to the IAA degradation pathway. The *iacA* gene product is believed to carry out one of the first steps, based on its ability to convert indole to indoxyl, which can dimerize to form the blue pigment indigo (Alemayehu *et al.* 2004). This activity has been reported for the *iacA* ortholog *idoA* from *Pseudomonas alcaligenes* PA-10 (Alemayehu *et al.* 2004), and *iacA* from *A. baumannii* ATCC 19606 (Lin *et al.* 2012). The involvement of other *iac* genes in the IAA degradation pathway remains more speculative. A transposon insertion into the *iacH* gene abolished IAA degradation by *P. putida* 1290 (Leveau and Gerards 2008), and this defect could be restored only by complementation by both *iacH* and the downstream *iacI* gene (Leveau and Gerards 2008). Collectively, the *iac* genes are thought to code for the conversion of IAA to catechol or a precursor, given that insertional inactivation of the *cat* and *pca* genes abolished the ability of *P. putida* 1290 to grow on IAA (Leveau and Gerards 2008). These *cat* and *pca* genes encode the enzymatic, multi-step catalysis of catechol into ß-ketoadipate. There is some evidence that *iac* gene expression is inducible. In *A. baumannii* ATCC 19606, the IacA protein was detected by Western blotting in cells cultured on IAA but not in cells on pyruvate (Lin *et al.* 2012). Extracts of IAA-grown cells of *P. putida* 1290 showed elevated levels of catechol 1,2-dioxygenase activity (Leveau and Lindow 2005), suggesting a coordinated regulation of *iac* genes and downstream *cat* and *pca* genes. The involvement of the *iacR* gene in the inducibility of the IAA degradation pathway remains unknown. *IacR* is one of the genes on the *iac* gene cluster and predicted to encode a MarR-type transcriptional regulator (Leveau and Gerards 2008).

Here, we report on our continued efforts to link the *iac* gene cluster to the IAA degradative phenotype, with the long-term goal to render a more complete understanding of the function of *iac* genes and their ecological role. Using the model strain *P. putida* 1290, we demonstrate the inducibility of *iac* gene expression in response to IAA, explore the contribution of individual *iac* genes to the IAA degradative phenotype, and identify several intermediates in the IAA degradation pathway. Furthermore, taking advantage of heterologous expression of *iac* genes in the non-IAA degrader *P. putida* KT2440, we present evidence for the chemotactic behavior of *P. putida* 1290 towards IAA.

Methods and Materials

Bacterial Strains and Growth Conditions Table 1 lists all the bacterial strains used in this study. Strains of *Pseudomonas putida* were grown at 30 °C on either Lysogeny Broth (LB), King's B (King *et al.* 1954), or M9 minimal medium (Sambrook *et al.* 1989) that was supplemented with 6.58 μM FeSO$_4$ and 8.33 mM glucose, 5 mM indole-3-acetic acid (IAA) (Sigma Aldrich, St. Louis, MO, USA), 8.3 mM benzoate, or 8.33 mM sodium citrate. *Escherichia coli* strains were grown at 37 °C on LB or M9 minimal medium supplemented with FeSO$_4$, glucose, thiamine, and leucine at concentrations of 6.58 μM, 8.33 mM, 10 μg ml^{-1}, and 100 μg ml^{-1}, respectively. Strains grown in liquid media were routinely incubated in the dark on an orbital shaker at 275 rpm to provide sufficient aeration. Growth media were supplemented with antibiotics as appropriate at the following final concentrations: kanamycin, 50 μg ml^{-1} (Km$_{50}$); tetracycline, 15 μg ml^{-1} (Tc$_{15}$); ampicillin, 50 μg ml^{-1} (Amp$_{50}$); or rifampicin 40 μg ml^{-1} (Rif$_{40}$).

Plasmid DNA Isolation, Manipulation, and Transformation Plasmids used in this study are listed in Table 1. Plasmid DNA was isolated from overnight bacterial cultures using a GeneJet Plasmid Miniprep Kit (Fermentas Thermo Scientific, Waltham, MA, USA), quantified with a NanoDrop (Thermo Scientific, Waltham, MA, USA), and checked for quality by agarose gel electrophoresis and GelRed staining (Biotium, Hayward, CA, USA). Plasmid DNA was digested with restriction enzymes as recommended by the manufacturer, and DNA fragments were recovered from excised agarose gel slices by using the QIAquick Gel Extraction Kit (QIAGEN, Germantown, MD, USA). Ligation reactions were incubated with T4 DNA ligase (Fermentas) at room temperature for 1 h, then heat-inactivated for 10 min at 65 °C. Non-compatible ends were blunted using a Quick Blunting Kit (New England BioLabs, Ipswich, MA, USA) prior to ligation. Chemically competent *E. coli* TOP10 cells (Life Technologies, Carlsbad, CA, USA) were transformed with 5 μl of the ligation reaction. For the transformation of *P. putida* or *E. coli* with purified plasmid DNA, we prepared electrocompetent cells and used 50 ng of DNA, as described previously (Leveau and Gerards 2008). Electroporation was performed with a Gene Pulser Xcell Microbial System (Bio-Rad, Hercules, CA, USA), using the manufacturer's settings for *E. coli* or *Pseudomonas aeruginosa* as needed. A recovery period of 1 hr for *E. coli* or 2 hr for *P. putida* occurred in 1 ml of SOC (Sambrook

Table 1 Bacterial strains, plasmids and primers used in this study

Strain	Description	Relevant phenotype	Source
P. putida 1290R	original source of the *iac* gene cluster	Rif_{40}	(Leveau and Lindow 2005)
P. putida KT2440R	not able to use IAA as a carbon source	Rif_{40}	(Nelson *et al.* 2002)
E. coli TOP10	general *E. coli* host for plasmids	Km^S, Tc^S	Invitrogen
E. coli BW15113	wild type indole production		(Lee *et al.* 2007)
E. coli BW15113Δ*tnaA*	reduced indole production		(Lee *et al.* 2007)
E. coli BW15113Δ*trpL*	increased indole production		(Lee *et al.* 2007)

Plasmid	Description	Antibiotic Resistance	Source
pCC1FOSEcoAscPLUS	source of *iac* genes	$Cm_{12.5}$	(Leveau and Gerards 2008)
pME6031	broad-host range vector	Tc_{15}	(Heeb *et al.* 2000)
pPROBE'-gfp[tagless]	Km control plasmid	Km_{50}	(Miller *et al.* 2000)
pIAC113	9.4-kb *Hind*III/*Sac*I fragment of pCC1FOSEcoAscPLUS in pME6031	Tc_{15}	this paper
pIAC115	derivative of pIAC113	Tc_{15}	this paper
pIAC115-vector::Tn*5*	pIAC115 with Tn*5* insertion in vector	Km_{50} Tc_{15}	this paper
pIAC115-*iacA*::Tn*5*	pIAC115 with Tn*5* insertion in *iacA*	Km_{50} Tc_{15}	this paper
pIAC115-*iacB*::Tn*5*	pIAC115 with Tn*5* insertion in *iacB*	Km_{50} Tc_{15}	this paper
pIAC115-*iacC*::Tn*5*	pIAC115 with Tn*5* insertion in *iacC*	Km_{50} Tc_{15}	this paper
pIAC115-*iacD*::Tn*5*	pIAC115 with Tn*5* insertion in *iacD*	Km_{50} Tc_{15}	this paper
pIAC115-*iacE*::Tn*5*	pIAC115 with Tn*5* insertion in *iacE*	Km_{50} Tc_{15}	this paper
pIAC115-*iacF*::Tn*5*	pIAC115 with Tn*5* insertion in *iacF*	Km_{50} Tc_{15}	this paper
pIAC115-*iacG*::Tn*5*	pIAC115 with Tn*5* insertion in *iacG*	Km_{50} Tc_{15}	this paper
pIAC115-*iacH*::Tn*5*	pIAC115 with Tn*5* insertion in *iacH*	Km_{50} Tc_{15}	this paper
pIAC115-*iacR*::Tn*5*	pIAC115 with Tn*5* insertion in *iacR*	Km_{50} Tc_{15}	this paper
pIAC115-Δ*iac*	pIAC115-vector::Tn*5*-Δ*iacABCDEFGRHI*	Km_{50} Tc_{15}	this paper
pIAC115-*iacAB*	pIAC115-vector::Tn*5*-Δ*iacCDEFGRHI*	Km_{50} Tc_{15}	this paper
pCR4Blunt-TOPO-04-A3	genome fragment *P. putida* 1290R with *iacA*	Km_{50}	(Leveau and Gerards 2008)
pCR4Blunt-TOPO-04-A4	genome fragment *P. putida* 1290R with *iacA*	Km_{50}	(Leveau and Gerards 2008)
pCR4Blunt-TOPO-04-D3	genome fragment *P. putida* 1290R with *iacA*	Km_{50}	(Leveau and Gerards 2008)
pCR4Blunt-TOPO-04-G10	genome fragment *P. putida* 1290R with *iacA*	Km_{50}	(Leveau and Gerards 2008)

Primer	Description	Amplicon Size	Sequence (5′→3′)
iacA_F	expression of *iacA*	99 bp	GTTCGATCGCCAGCGCCACATTTC
iacA_R			TCCAGTCCACCGAAGCGTTTTGGCA
iacC_F	expression of *iacC*	112 bp	ATCTCGGTCACGGAAACGGAAATC
iacC_R			CCATCGGGCCCTGGAAGTGTT
iacH_F2	expression of *iacH*	70 bp	GCGGCGTGTTCGGGCTCAA
iacH_R2			CTGGTACGCGCAGGCATCACG
iacR_F	expression of *iacR*	117 bp	CGTCGAGGTCGATCTTCTTGAGCAGAC
iacR_R			ACGACCCGGCCAGCGATGAAT
cbrA_F	expression of *cbrA*	121 bp	CACACGCCACTGCAGGAAGGTC
cbrA_R			CCAGCGAGCGCGGGTTGA
benC_F	expression of *benC*	101 bp	GGCCGCGCAGATCCCCAACTT
benC_R			GGCCCGGCGCGATGTGCT
1290 16S_F1	expression of *benC*	104 bp	GTCCACGCCGTAAACGATGTCAAC
1290 16S_R1			CGTACTCCCCAGGCGGTCAACTT
pIAC115-F	for construction pIAC115	1,516 bp	GTGAAGCTTGGACGCTAGGGCAGGG
pIAC115-R			CTTCGTTCCGGTGGGCCC
KAN2-RP-1	Tn*5* sequencing primer	n/a	GCAATGTAACATCAGAGATTTTGAG
KAN2-FP-1			ACCTACAACAAAGCTCTCATCAACC

et al. 1989) on an orbital shaker. Transformants were selected on the appropriate agar medium.

Construction of pIAC115 and its Derivatives A cluster of ten *iac* genes involved in the bacterial mineralization of IAA was cut from the vector pCC1FOS11EcoAscPLUS (Leveau and Gerards 2008) as a 9.4-kb *Hin*dIII/*Sac*I fragment. This region of DNA was ligated into the 8.3-kb *Hin*dIII/*Sac*I-digested backbone of pME6031 (Heeb *et al.* 2000) to produce pIAC113. This plasmid was used as a template in a PCR with primers pIAC115-F and pIAC115-R (Table 1) to amplify a 1.5-kb fragment that was cut with *Hin*dIII and *Mau*BI and ligated into *Hin*dIII/*Mau*BI-digested pIAC113 to generate pIAC115. This plasmid then was used in an *in vitro* EZ-Tn*5*<KAN-2>Tnp Transposome kit (Epicentre, Madison, WI, USA) as per the manufacturer's instructions, and transformed into *E. coli* TOP10. From 48 transformants, plasmid DNA was isolated and sent to the CBS UC DNA Sequencing Facility (UC Davis, CA, USA) for sequencing with the primer KAN-2-FP, which is designed to read from the transposon into the flanking plasmid DNA. DNA sequences were analyzed using the MegAlign and Seqbuilder modules of the Lasergene software (DNASTAR, Madison, WI, USA) to determine the transposon insertion site for each sequenced clone. Ten pIAC115::Tn*5* plasmids were selected for further study: nine carrying the transposon inserted in a unique *iac* gene (pIAC115-*iacX*::Tn*5*, where *X* represents *A, B, C, D, E, F, G, R,* or *H*; we never recovered a plasmid carrying Tn*5* in *iacI*) and one carrying the transposon in the vector backbone of pIAC115 (pIAC115-vector::Tn*5*). The latter plasmid was also used to construct the three deletion derivatives pIAC115-vector::Tn*5*-Δ*iacABCDEFGRHI* and -Δ*iacCDEFGRHI*, by deletion of a 9.0-kb *Hin*dIII-*Eco*RI or 7.0-kb *Bsr*GI-*Eco*RI internal fragment, respectively.

Characterization of E. coli and P. putida Strains Carrying pIAC115::Tn5 Plasmids To assess the contribution of *iac* genes to IAA degradation, cells of *E. coli* TOP10 or *P. putida* KT2440 carrying pIAC115::Tn*5* plasmids were grown in LB Tc$_{15}$ supplemented with 5 mM IAA for 18 h on an orbital shaker. One-ml aliquots were centrifuged at 10,000×g for 30 sec, and IAA concentrations were determined using Salkowski reagent as described previously (Leveau and Gerards 2008). To assess the contribution of the *iac* genes in the utilization of IAA as a source of carbon and energy, cells of *P. putida* KT2440 carrying pIAC115::Tn*5* plasmids were inoculated in liquid M9 Tc$_{15}$ medium supplemented with 5 mM IAA. To assess indigo production of *E. coli* BW25113, *E. coli* BW25113Δ*tnaA*, and *E. coli* BW25113Δ*trpL* (Lee *et al.* 2007) carrying selected pIAC115::Tn*5* plasmids, strains were streaked onto LB Km$_{50}$ agar, with or without a few crystals of indole (Sigma Aldrich) in the plastic lid of the inverted petri plates, at 30 °C for 3 days.

Transcriptional Profiling of iac Genes Relative levels of *iac* gene expression in *P. putida* 1290R were quantified by quantitative reverse-transcriptase (RT) real-time PCR. The PrimerSelect module of Lasergene (DNASTAR) was used to design primers that would amplify unique fragments, between 70 and 121 bp in size and internal to different *iac* genes, the 16S rRNA reference gene, or *benC* and *cbrA* control genes (Table 1). Cells were grown as overnight cultures in KB Rif$_{40}$ or KB Rif$_{40}$ supplemented with 5 mM IAA, harvested by centrifugation at 8,000×g for 2 min, washed in 1× M9 minimal salts, and transferred to a sterile 125 ml Erlenmeyer flask as a 1/100 dilution into 20 ml of M9 minimal medium supplemented with 6.58 μM FeSO4 and one or more carbon sources. At mid-exponential phase, approximately $2×10^8$ cells were harvested, mixed with two volumes of RNAprotect (QIAGEN), and RNA was extracted using a RNeasy Mini Kit (QIAGEN) with the optional on-column DNAse step. RNA was eluted in 50 μl water twice, quantified by NanoDrop, and quality-checked on a 1 % agarose gel in 1X TAE. One μg of RNA was used as the template for synthesis of cDNA using the Super Script III First-Strand Synthesis Super Mix for qRT-PCR (Invitrogen Life Technologies, Carlsbad, CA, USA) with the following conditions: 10 min at 25 °C, 30 min at 50 °C, 5 min at 85 °C, followed by chilling on ice. To remove RNA, 2U *E. coli* RNase H was added to each preparation and incubated at 37 °C for 20 min. Fifty pg of template cDNA were mixed with 12.5 μM each of forward and reverse primer in 1x Fast SYBR Green Master Mix (Invitrogen Life Technologies), and run on an Applied Biosystems 7500 Fast Real-Time PCR System (Life Technologies) using the following settings: 10 min at 95 °C, followed by 40 cycles of 15 sec at 95 °C and 1 min at 60 °C. For the standard curves, we generated amplicons for each target gene in a standard PCR using 20 ng of *P. putida* 1290 genomic DNA that was isolated using a Blood and Tissue DNeasy kit (QIAGEN). PCR primers and unused nucleotides were removed with an UltraClean PCR Clean-Up Kit (Mo Bio Laboratories, Carlsbad, CA, USA). Standard curves were derived from real-time PCRs on ten-fold dilution series (0.002–2 pg range) of each purified amplicon. The relative expression ratio R of individual target genes was calculated as $E_{target}^{\Delta CP target(control-sample)}/E_{ref}^{\Delta CP ref(control-sample)}$ (Pfaffl 2001) in which E_{target} is the real-time efficiency of the target gene, E_{ref} the real-time efficiency of the 16S rRNA reference gene, ΔCP is the difference in crossing point (or C_t), and 'control' refers to growth on M9 with citrate as the carbon source.

Gas Chromatography and Mass Spectrometry (GC-MS) Selected *E. coli* TOP10 (pIAC115::Tn*5*) strains were precultured in LB Km$_{50}$, pelleted by centrifugation, inoculated as a 1/100 dilution into M9 Km$_{50}$ minimal medium containing glucose, thiamine, and leucine, in addition to 200 μM IAA, and grown for 24 h at 37 °C with shaking at 275 rpm. As a control, we used medium that was not inoculated with cells. Aliquots (2 ml) were centrifuged and 1.5 ml of supernatant was filtered through a

sterile 0.2-μm Puradisc 25 AS disposable filter (Whatman, Florham Park, NJ, USA), and frozen at −20 °C until sent to the UC Davis Metabolomics core facility for trimethylsilyl (TMS)-derivatization and GC-MS analysis as described elsewhere (Fiehn *et al.* 2008). In total, 218 compounds were identified, of which 106 could be annotated using BinBase (Fiehn *et al.* 2005). Fragmentation profiles for each of the candidate compounds were examined using AMDIS software (Stein 1999) to infer putative structures.

Chemotaxis Experiments A soft agar plate assay (Harwood *et al.* 1994) was used to evaluate the ability of *P. putida* 1290R-carrying plasmid pPROBE'-gfp[tagless] (Miller *et al.* 2000) and *P. putida* KT2440R carrying plasmid pIAC115-vector::Tn*5* to chemotaxi towards IAA. Soft agar plates (94-mm diam) contained 0.3 % agar, M9 Km$_{50}$ medium supplemented with 6.58 μM FeSO$_4$, and either 5 mM IAA, 8.3 mM sodium benzoate, or no carbon source. Single colonies of each strain were grown overnight in 3 ml LB Km$_{50}$ with shaking at 30 °C, and a 5-μl aliquot was placed in the center of each soft agar plate. After incubation at 30 °C for 16 h, the diameters of bacterial spread were measured and compared.

Results

IAA-Induced Expression of iac Genes Quantitative RT real-time PCR analysis of RNA extracted from *P. putida* 1290 cultures revealed that on mineral medium, with IAA as the sole source of carbon and energy, the expression of *iacA* and *iacC* was >2 orders of magnitude greater than with glucose (Fig. 1). In the presence of both glucose and IAA, *iacA* and *iacC* expression levels were lower than with IAA only, but still well above those with glucose alone, suggesting that *iac* genes are not subject to catabolite repression. For *iacH* and *iacR*, we also observed elevated expression on IAA and on glucose plus IAA, albeit to a lower level. We did not observe IAA-induced expression of *cbrA*, which is predicted to be involved in IAA sensing (Leveau and Gerards 2008), nor did we see induction of *iac* gene expression when the cells were grown on benzoate (Fig. 1). Conversely, the *benC* gene, which contributes to growth on benzoate (Leveau and Gerards 2008), was induced by benzoate but not IAA (Fig. 1).

Characterization of P. putida and E. coli Strains Carrying pIAC115::Tn5 Plasmids The plasmid pIAC115 carries the complete *iac* gene cluster in the broad-host vector pME6031 (Fig. 2a). *In vitro* transposon mutagenesis of this plasmid and flank-sequencing of insertion sites revealed 29 derivatives of pIAC115 that carried the transposon in one of the *iac* genes. Nine of these were selected for further study, representing insertions in *iacA, iacB, iacC, iacD, iacE, iacF, iacG, iacR,*
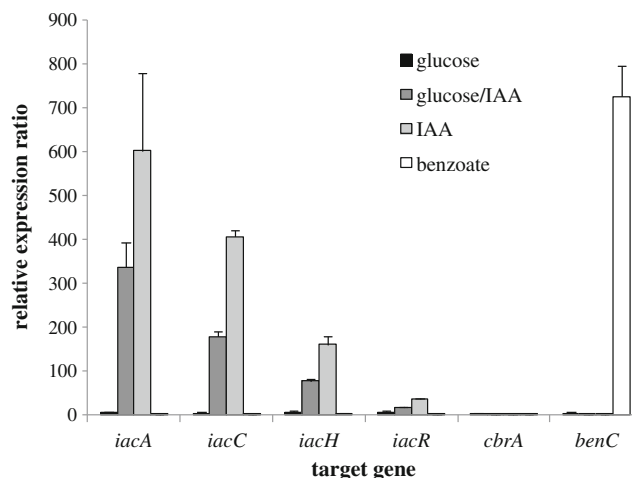
Fig. 1 Indole-3-acetic acid (IAA)-induced expression of *iac* genes. Shown is the relative expression ratio (R) of 6 target genes (*iacA, iacC, iacH, iacR, cbrA,* and *benC*) for cultures of *Pseudomonas putida* 1290R that were grown on mineral medium containing different carbon sources (glucose, glucose plus IAA, IAA, or benzoate). R was calculated using the 16S rRNA gene as a reference gene and citrate as the control carbon source. Error bars indicate standard deviations of the means of technical replicates within this representative biological experiment

and *iacH*, so as to assess the individual role of these genes in IAA degradation. Also included was derivative pIAC115-vector::Tn*5*, which carries a transposon insertion outside of the *iac* gene cluster. In addition, we constructed two deletion derivatives of pIAC115-vector::Tn*5*: one by removal of the entire *iac* gene cluster to give pIAC115-Δ*iac,* and the other by removal of *iacCDEFGRHI* to generate pIAC115-*iacAB*. *P. putida* KT2440 or *E. coli* TOP10 were transformed with derivatives of pIAC115 and tested for various phenotypes. The results are summarized in Table 2 and described in the next paragraphs.

Introduction of pIAC115-vector::Tn*5* (complete *iac* gene cluster) into *P. putida* KT2440 conferred the ability to grow on IAA as the sole source of carbon and energy. Insertional inactivation of *iacA, iacC, iacD, iacE* or *iacH,* but not *iacF, iacG,* or *iacR,* completely abolished this phenotype. *E. coli* TOP10 carrying pIAC115-vector::Tn*5* did not gain the ability to grow at the expense of IAA. However, this strain was able to make IAA disappear during growth on glucose plus IAA. This ability was lost with insertional inactivation of *iacA* or with removal of the entire *iac* gene cluster. *E. coli* TOP10 carrying an insertion in any one of the other *iac* genes or carrying pIAC115-*iacAB* showed the same capability of IAA destruction as *E. coli* (pIAC115-vector::Tn*5*). When grown in LB plus IAA, cultures of *E. coli* (pIAC115-vector::Tn*5*) turned brown after overnight incubation. A similar observation was made for *E. coli* strains carrying pIAC115-*iacF*::Tn*5*, -*iacG*::Tn*5*, and -*iacR*::Tn*5*. We suspect that the brown color results from the polymerization of catechol that accumulates in the supernatant (see GC-MS analysis below) and which *E. coli* is unable to metabolize
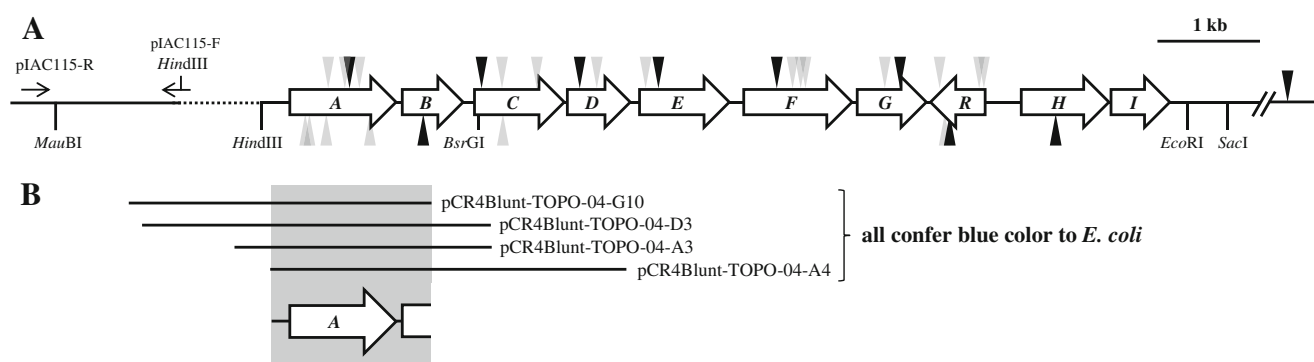
Fig. 2 **a** Diagram showing part of plasmid pIAC115 carrying the *iac* gene cluster and the location of 30 EZ-Tn*5*<KAN-2>transposon insertion events. Each insertion event is represented by a triangle: down- or upward direction of the triangles correspond to right or left orientations, respectively, of the transposed KAN-2 gene. The ten insertions labeled with a solid black triangle were selected for subsequent experiments. Of these, nine are in one of the *iac* genes and one in the vector backbone. The stippled line represents a DNA fragment that shows homology to

the Tn*5*<KAN-2>sequence and was removed from pIAC113 to create pIAC115 using primers pIAC115-F and pIAC115-R. **b** Relative size and overlap of DNA inserts in four pCR4Blunt-TOPO plasmids from the original shotgun clone library of *Pseudomonas putida* 1290 genomic DNA (Leveau and Gerards 2008). All four conferred a blue color to colonies of host *E. coli* DH5α. They share a 1,568-bp fragment harboring the *iacA* gene

further. We note that these three plasmids and pIAC115-vector::Tn*5* were the only ones to confer growth on IAA to *P. putida* KT2440, suggesting that *iac*-encoded growth on IAA is linked to the ability to metabolize catechol.

On LB agar plates, colonies of *E. coli* TOP10 harboring plasmid pIAC115-*iacAB* or pIAC115-*iacR*::Tn*5* developed a blue color. None of the other pIAC115 derivatives conferred this property (Table 2). The pIAC115-*iacR*::Tn*5*-induced blue

Table 2 Functional characterization of pIAC115 derivatives in *Pseudomonas putida* and *Escherichia coli*

Plasmid	Growth[a]	Destruction[b]	Brown[c]	Blue[d]	IAA[e]	#1[e]	#2[e]	#3[e]
pIAC115-vector:: Tn*5*[f]	+	+	+	-	-	-	+	+
pIAC115-*iacA*::Tn*5*	-	-	-	-				
pIAC115-*iacB*::Tn*5*	-	+	-	-				
pIAC115-*iacC*:: Tn*5*	-	+	-	-	+/−	-	+	-
pIAC115-*iacD*:: Tn*5*	-	+	-	-				
pIAC115-*iacE*:: Tn*5*	-	+	-	-	-	+	-	-
pIAC115-*iacF*:: Tn*5*	+	+	+	-				
pIAC115-*iacG*:: Tn*5*	+/−	+	+/−	-				
pIAC115-*iacR*:: Tn*5*	+	+	+	+				
pIAC115-*iacH*:: Tn*5*	-[g]	+	-	-				
pIAC115-Δ*iac*	-	-	-	-	+	-	-	-
pIAC115-*iacAB*	-	+	-	+	+/−	+	-	-

[a] *P. putida* KT2440R in M9 Km$_{50}$ liquid medium supplemented with 5 mM IAA as sole carbon and energy source. A + sign means that bacterial biomass was produced as measured by optical density measurements at 600 nm. A - sign means that no bacterial growth was observed

[b] *E. coli* TOP10 in M9 liquid medium supplemented with glucose and 5 mM IAA; Salkowski-based IAA detection after overnight incubation. A - sign means that IAA remained untouched by the bacteria. A + sign means that IAA had completely disappeared from the medium

[c] *E. coli* TOP10 in LB Km$_{50}$ supplemented with 5 mM IAA incubated overnight on an orbital shaker. A + sign means that the medium had visibly colored brown, while such browning of the medium was not obvious for samples labeled with a − sign

[d] Blue pigment formation by colonies of *E. coli* TOP10 on LB Km$_{50}$ agar

[e] *E. coli* TOP10 on M9 glucose plus 0.2 mM IAA; GC-MS-based detection of IAA and compounds #1 (putatively annotated as 5-hydroxy-IAA, but possibly 2-OH-IAA), #2 (possibly diOxIAA), and #3 (catechol). Ion counts for each of the compounds are given in Supplemental Figure 1. Mass spectra of compounds #1, #2, and #3 and corresponding BinBase library spectra, if applicable, are shown in Supplemental Figure 2

[f] Full *iac* gene cluster

[g] With formation of brown color

colony phenotype also was observed with the host strain *E. coli* BW25113 (Fig. 3). When introduced into *E. coli* BW25113 Δ*tnaA*, which has reduced indole production (Lee *et al.* 2007), pIAC115-*iacR*::Tn5 failed to produce the blue color, but pigment production could be restored to wildtype levels by exogenously providing indole (Fig. 2). A Δ*trpL* derivative of BW25113 that overproduces indole (Lee *et al.* 2007) showed blue color formation similar to wildtype. These results suggest that the blue color is produced from indole by a *iacAB*-encoded activity that is repressed by *iacR*. During the shotgun sequencing of the *iac* gene cluster of *P. putida* 1290 (Leveau and Gerards 2008), four library clones were observed to produce a similar blue color. Sequence of the inserts revealed that they shared the *iacA* gene (Fig. 2b), suggesting the *iacA* gene product is the catalyst for pigment formation and that *iacB* is not needed.

*Intermediates of the iac-Directed IAA Degradation Pathway*
GC-MS analyses were performed on the supernatants of *E. coli* strains carrying different pIAC115 derivatives (full *iac* gene cluster, pIAC115-*iacC*::Tn5, -*iacE*::Tn5, -Δ*iac*, or -*iacAB*), after overnight growth on mineral medium containing glucose supplemented with 0.2 mM IAA. Authentic IAA was identified based on a BinBase-annotated parent ion with m/z 319 (IAA-2TMS), as well as a strong daughter peak at m/z 202, which likely resulted from loss of the trimethylsilylated carboxylic acid group on the IAA side chain. IAA was near the detection limit in the supernatants of *E. coli* carrying pIAC115-vector::Tn5 (the full *iac* gene cluster) and pIAC115-

iacE::Tn5 (transposon insertion in *iacE*), while the level of IAA in the supernatants of cells carrying the empty vector (pIAC115-Δ*iac*) was similar to that of the no-cells-added control. Supernatants of *E. coli* (pIAC115-*iacC*::Tn5) and *E. coli* (pIAC115-*iacAB*) showed residual concentrations of IAA.

We identified three compounds that accumulated differently in the supernatants of the tested *E. coli* strains by GC-MS analysis (Table 2). Compound #3 was unambiguously identified as catechol, with an m/z 254 parent ion and daughter ions with m/z 136, 151, 166, and 239. Catechol only appeared in supernatants of cells carrying the complete *iac* cluster. Compound #1 was putatively annotated as 5-hydroxyindoleacetic acid (5-OH-IAA), using the ion peak at m/z 290 and lower intensity peaks at m/z 407 (5-OH-IAA-3TMS) and 202 for identification. This compound was found in the supernatants of *E. coli* (pIAC115-*iacE*::Tn5) and *E. coli* (pIAC115-*iacAB*). Compound #2 could not be annotated. It had a complex peak profile with signature ion peaks at m/z 202, 292, 306, 364, and 423. This compound appeared in the supernatants of cells carrying the full *iac* gene cluster as well as the plasmid pIAC115-*iacC*::Tn5.

Chemotaxis of P. putida 1290 towards IAA On soft agar plates containing IAA, *P. putida* 1290 exhibited chemotactic behavior, as demonstrated by the radial growth of the bacteria (Fig. 4). *P. putida* KT2440 carrying plasmid pIAC115-vector::Tn5 (complete *iac* gene cluster) did not show such behavior (Fig. 4), although it could utilize IAA as a sole source of carbon and energy (Table 2). This suggests that

Fig. 3 Production of indigo by *Escherichia coli* BW25113 strains carrying different pIAC115 derivatives. *E. coli* BW25113 Δ*tnaA* has been described as a strain with reduced indole production (compared to wildtype *E. coli* BW25113), whereas *E. coli* BW25113 Δ*trpL* is an overproducer of indole. Plasmid pIAC115 harbors the entire *iac* gene cluster, whereas pIAC115-*iacR*::Tn5 carries a transposon insertion in the *iacR* gene
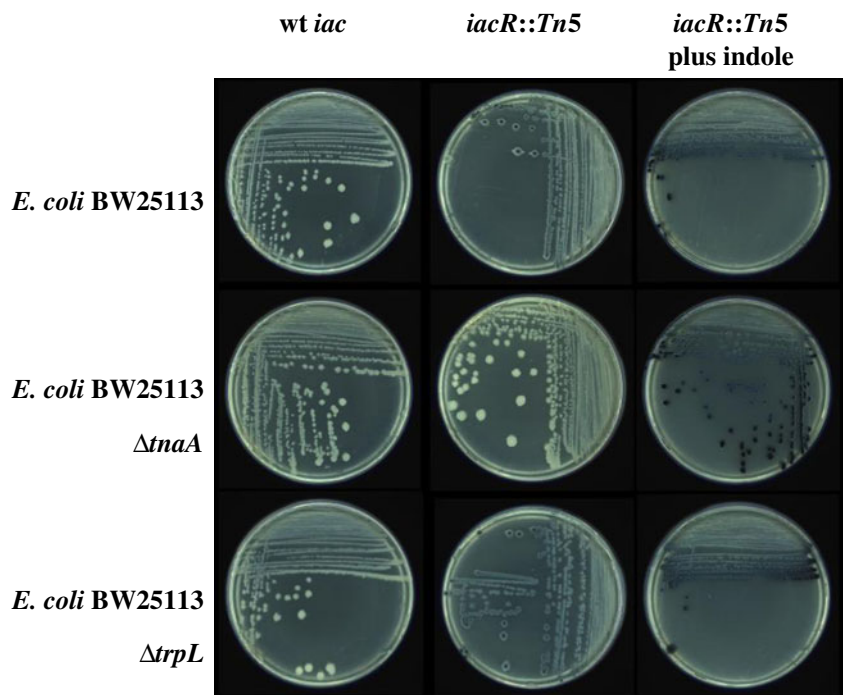
Fig. 4 Test of chemotactic behavior by *Pseudomonas putida* 1290 and *P. putida* KT2440 (pIAC115) towards indole-3-acetic acid (IAA). A drop of overnight culture was placed in the center of a M9 0.3 % agar plate containing benzoate, IAA, or no carbon source, incubated for 6 hr at 30 °C, and analyzed for outward spread of bacterial growth
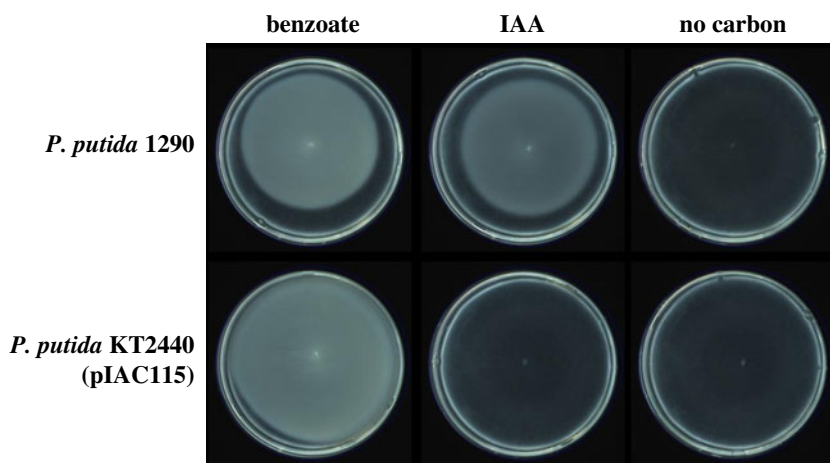
IAA catabolism alone is not sufficient for chemotaxis towards IAA. Figure 4 also shows a positive control (benzoate) and negative control (no carbon source) for chemotaxis.

Discussion

The experimental results we present here are consistent with the following model for *iac*-encoded catabolism of IAA. A knockout of *iacA* but none of the other genes in the *iac* gene cluster abolished the ability of *E. coli* to make IAA disappear (as measured by Salkowski staining), suggesting that *iacA* codes for the first step in the IAA degradation pathway. The *iacA* gene product also catalyzed blue pigment production in *E. coli*, which we showed to be dependent on the presence of indole. This suggests that *iacA* codes for the hydroxylation of position 3 of the indole ring to produce indoxyl (tautomeric with 3-oxindole), which in the presence of oxygen dimerizes to form indigo. We hypothesize that hydroxylation of IAA in the same position would yield either 3-oxindole with release of the acetic acid side chain, or 2-hydroxy-indole-3-acetic acid (2-OH-IAA) by migration of the hydroxyl group from position 3 to position 2 on the indole ring. 2-OH-IAA is a tautomer of OxIAA, which is a major degradation product of IAA in plants (Ljung *et al.*

2002). Published GC-MS analysis of silylated 2-OH-IAA (Ostin *et al.* 1998) showed ion peaks at *m/z* 290, as well as 407 and 202. This profile is very similar to what we found for compound #2, which BinBase annotated as 5-OH-IAA, which is an isomer of 2-OH-IAA/OxIAA. OxIAA is unreactive with Salkowski reagent (Reinecke and Bandurski 1981), whereas 5-OH-IAA produces a beige to brown color (Glickmann and Dessaux 1995). Given the absence of Salkowski-induced color formation in supernatants that harbored compound #1, we propose that compound #1 is in fact 2-OH-IAA. It accumulated in the supernatants of IAA-exposed *E. coli* cells carrying pIAC115-*iacAB* or pIAC115-*iacE*::Tn5 (Table 2). The *iacB* gene is not needed for blue pigment production (Fig. 2b) or for making IAA disappear, as determined by Salkowski reagent (Table 2), suggesting that the *iacA* gene product is sufficient to catalyze the conversion of IAA into 2-OH-IAA. The data also indicate that 2-OH-IAA might be the substrate for *iacE* in the IAA degradation pathway. We note that hydroxylation of 2-OH-IAA at position 3 of the indole ring would yield 3-hydroxy-2-oxindole-3-acetic acid (dioxindole-3-acetic acid, or diOxIAA), which has been proposed as an intermediate of IAA catabolism in the bacterium *Bradyrhizobium japonicum* (Jensen *et al.* 1995). A 3TMS-derivative of diOxIAA is predicted to have a parent ion with an *m/z* of 423, and loss of the COO-TMS would yield a 306 peak. These values are part of
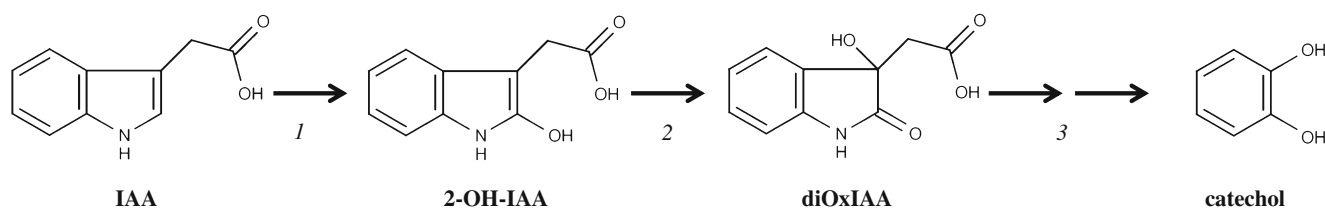
Fig. 5 Proposed pathway for *iac*-encoded degradation of indole-3-actic acid (IAA) in *Pseudomonas putida* 1290. Shown are three intermediates, one confirmed (catechol) and two suspected (2-hydroxy-IAA, or 2-OH-IAA; 3-hydroxy-2-oxo-IAA, or diOxIAA) based on GC-MS

analysis. Insertional inactivation experiments suggest that *iacA* is involved in step 1, *iacE* in step2 and *iacC* in step 3. The role of other *iac* genes (*iacB*, *iacD*, *iacE*, *iacF*, *iacG*, *iacH*, and *iacI*) in these steps remains unknown

the spectrum for compound #2, and so we tentatively propose that compound #2 is diOxIAA. It accumulated to the highest levels in the supernatants of *E. coli* cells carrying plasmid pIAC115-*iacC*::Tn*5*, but we also found it in cells carrying the full *iac* gene cluster. Possibly, this indicates that diOxIAA is the substrate for the *iacC* gene product, and that this reaction is the rate limiting step in the *iac*-encoded pathway of IAA degradation. Catechol (compound #3) was identified only in the supernatants of *E. coli* cells carrying the full *iac* cluster, indicating that it is the end product of the *iac*-encoded pathway. This is consistent with the observation that *P. putida* KT2440, which carries the *cat/pca* genes for catechol utilization, can grow on IAA when transformed with the *iac* gene cluster, while *E. coli*, which does not possess such genes, cannot. This also explains the accumulation in *E. coli* supernatants of catechol, which is known to polymerize to produce a brown color (Leveau and Gerards 2008). A tentative pathway for IAA degradation in *P. putida* 1290 is presented in Fig. 5. The roles of other *iac* genes in this pathway remain unknown. Based on gene synteny and sequence homology, it has been suggested (Leveau and Gerards 2008) that IacD is a subunit of the IacC protein. We suspect that the conversion of diOxIAA to catechol involves multiple steps that require the products of *iacF* and *iacG*. Our data show that a functional copy of these genes is not required to bestow upon *P. putida* KT2440 the ability to grow on IAA. On the genome of *P. putida* KT2440 (Nelson *et al.* 2002), we identified orthologs of *iacF* and *iacG* (NCBI accession numbers AAN69333 and AAN69243, respectively) that may be similar enough in function (based on sequence identity of 51 % and 28 %, respectively) to rescue the absence of *iacF* and *iacG* and allow IAA degradation.

We demonstrated that the *iac*-encoded degradation of IAA in *P. putida* 1290 involves IAA-inducible expression of the *iac* genes (Fig. 1). The experiments with plasmids pIAC115-*iacR*::Tn*5* and pIAC115-*iacAB* in *E. coli* show that in the absence of *iacR*, expression of *iacA* is induced, as deduced from *iacA*-catalyzed indigo production. This suggests that *iacR* is a repressor of *iacA* expression. IacR shows high amino acid sequence identity to members of the Multiple Antibiotic Resistance Regulator (MarR) family, many of which regulate the expression of genes involved in antibiotic resistance, stress responses, virulence, or catabolism of aromatic compounds (Perera and Grove 2010). In *Comamonas testosteroni*, the MarR homolog CbaR represses the *cbaABC* operon, which codes for the degradation of 3-chlorobenzoate (Providenti and Wyndham 2001). Repression is relieved when CbaR binds the ligand 3-chlorobenzoate, which causes a reduction in DNA binding affinity of CbaR to its operator sites in the *cbaA* promoter region. Interestingly, the DNA binding affinity of CbaR is enhanced upon binding with 3-hydroxy- or 3-carboxyl-benzoate. It was suggested that this represents a mechanism to prevent gratuitous induction of *cbaABC* (Providenti and Wyndham 2001). The ligand of *iacR* remains

to be identified, but IAA is a likely candidate. Based on results with *E. coli* (pIAC115-*iacB*::Tn*5*), we tentatively conclude that indole is not an inducer of *iacA* gene expression, otherwise we would have expected this strain to produce indigo, assuming that *iacA* is solely responsible for the conversion of indole to indoxyl.

To the best of our knowledge, this study offers the first demonstration of bacterial chemotaxis towards IAA. The mechanism underlying this property in *P. putida* 1290 will be a subject of future investigations. Most likely, it involves one or more methyl-accepting proteins (MCPs), which are chemoreceptors that recognize a specific attractant and transmit a signal to the flagellar machinery (Krell *et al.* 2011). We can assume that an MCP-based chemotaxis towards IAA would involve a certain degree of specificity in *P. putida* 1290, since none of the 27 MCPs or MCP-like proteins identified on the genome of *P. putida* KT2440 (Parales *et al.* 2013) appeared to be able to surrogate and to induce chemotactic behavior toward IAA in *P. putida* KT2440 carrying the full *iac* gene cluster (Fig. 4). The knowledge that bacteria have the capability to chemotaxi towards IAA implies that this property is of use to these bacteria and offers a selective advantage to their survival. Many chemotactic behaviors are linked to metabolism of the attractant (Krell *et al.* 2011), and so bacteria like *P. putida* 1290 would have a competitive advantage over IAA-mineralizing bacteria that lack chemotactic capability. Another potential benefit is that bacteria can actively move towards biological sources of IAA. These might be plants (Cho *et al.* 2007), but also microbial producers of IAA, such as bacteria or fungi (Spaepen *et al.* 2007). Certain environments such as the plant leaf surface (Enya *et al.* 2007) are ubiquitously colonized by IAA-producing bacteria, and possibly, bacterial chemotaxis towards bacterially-produced IAA could contribute to the aggregative colonization patterns that are observed in such environments (Monier and Lindow 2004).

References

Alemayehu D, Gordon LM, O'Mahony MM, O'Leary ND, Dobson AD (2004) Cloning and functional analysis by gene disruption of a novel gene involved in indigo production and fluoranthene metabolism in *Pseudomonas alcaligenes* PA-10. FEMS Microbiol Lett 239:285–293

Cho M, Lee OR, Ganguly A, Cho HT (2007) Auxin-signaling: short and long. J Plant Biol 50:79–89

Dodd IC, Zinovkina NY, Safronova VI, Belimov AA (2010) Rhizobacterial mediation of plant hormone status. Annal Appl Biol 157:361–379

Enya J, Shinohara H, Yoshida S, Negishi TTH, Suyama K, Tsushima S (2007) Culturable leaf-associated bacteria on tomato plants and their potential as biological control agents. Microb Ecol 53:524–536

Faure D, Vereecke D, Leveau JHJ (2009) Molecular communication in the rhizosphere. Plant Soil 321:279–303

Fiehn O, Wohlgemuth G, Scholz M (2005) Setup and annotation of metabolomic experiments by integrating biological and mass spectrometric metadata. Data Integr Life Sci Proc 3615:224–239

Fiehn O, Wohlgemuth G, Scholz M, Kind T, Lee DY, Lu Y, Moon S, Nikolau B (2008) Quality control for plant metabolomics: reporting MSI-compliant studies. Plant J 53:691–704

Garcia-Gomez E, Gonzalez-Pedrajo B, Camacho-Arroyo I (2013) Role of sex steroid hormones in bacterial-host interactions. Biomed Res Int 2013:928290

Glickmann E, Dessaux Y (1995) A critical examination of the specificity of the Salkowski reagent for indolic compounds produced by phytopathogenic bacteria. Appl Environ Microbiol 61:793–796

Gray WM (2004) Hormonal regulation of plant growth and development. PLoS Biol 2:E311

Harwood CS, Nichols NN, Kim MK, Ditty JL, Parales RE (1994) Identification of the pcaRKF gene cluster from Pseudomonas putida: involvement in chemotaxis, biodegradation, and transport of 4-hydroxybenzoate. J Bacteriol 176:6479–6488

Heeb S, Itoh Y, Nishijyo T, Schnider U, Keel C, Wade J, Walsh U, O'Gara F, Haas D (2000) Small, stable shuttle vectors based on the minimal pVS1 replicon for use in gram-negative, plant-associated bacteria. Mol Plant Microbe Interact 13:232–237

Jensen JB, Egsgaard H, Vanonckelen H, Jochimsen BU (1995) Catabolism of indole-3-acetic acid and 4-chloroindole-3-acetic and 5-chloroindole-3-acetic acid in Bradyrhizobium japonicum. J Bacteriol 177:5762–5766

King EO, Ward MK, Raney DE (1954) Two simple media for the demonstration of pyocyanin and fluorescein. J Lab Clin Med 44:301–307

Krell T, Lacal J, Munoz-Martinez F, Reyes-Darias JA, Cadirci BH, Garcia-Fontana C, Ramos JL (2011) Diversity at its best: bacterial taxis. Environ Microbiol 13:1115–1124

Lee JT, Jayaraman A, Wood TK (2007) Indole is an inter-species biofilm signal mediated by SdiA. BMC Microbiol 7:15

Leveau JHJ, Gerards S (2008) Discovery of a bacterial gene cluster for catabolism of the plant hormone indole 3-acetic acid. FEMS Microbiol Ecol 65:238–250

Leveau JHJ, Lindow SE (2005) Utilization of the plant hormone indole-3-acetic acid for growth by Pseudomonas putida strain 1290. Appl Environ Microbiol 71:2365–2371

Lin GH, Chen HP, Huang JH, Liu TT, Lin TK, Wang SJ, Tseng CH, Shu HY (2012) Identification and characterization of an indigo-producing oxygenase involved in indole 3-acetic acid utilization by Acinetobacter baumannii. A Van Leeuw J Microb 101:881–890

Ljung K, Hull AK, Kowalczyk M, Marchant A, Celenza J, Cohen JD, Sandberg G (2002) Biosynthesis, conjugation, catabolism and homeostasis of indole-3-acetic acid in Arabidopsis thaliana. Plant Mol Biol 50:309–332

Miller WG, Leveau JHJ, Lindow SE (2000) Improved gfp and inaZ broad-host-range promoter-probe vectors. Mol Plant Microbe Interact 13:1243–1250

Monier JM, Lindow SE (2004) Frequency, size, and localization of bacterial aggregates on bean leaf surfaces. Appl Environ Microbiol 70:346–355

Nelson KE, Weinel C, Paulsen IT, Dodson RJ, Hilbert H, dos Santos VAPM, Fouts DE, Gill SR, Pop M, Holmes M et al (2002) Complete genome sequence and comparative analysis of the metabolically versatile Pseudomonas putida KT2440. Environ Microbiol 4:799–808

Ostin A, Kowalyczk M, Bhalerao RP, Sandberg G (1998) Metabolism of indole-3-acetic acid in Arabidopsis. Plant Physiol 118:285–296

Parales RE, Luu RA, Chen GY, Liu X, Wu V, Lin P, Hughes JG, Nesteryuk V, Parales JV, Ditty JL (2013) Pseudomonas putida F1 has multiple chemoreceptors with overlapping specificity for organic acids. Microbiology Published online ahead of print(doi: 10.1099/mic.0.065698-0)

Patten CL, Glick BR (1996) Bacterial biosynthesis on indole-3-acetic acid. Can J Microbiol 42:207–220

Perera IC, Grove A (2010) Molecular mechanisms of ligand-mediated attenuation of DNA binding by MarR family transcriptional regulators. J Mol Cell Biol 2:243–254

Pfaffl MW (2001) A new mathematical model for relative quantification in real-time RT-PCR. NAR 29:e45

Providenti MA, Wyndham RC (2001) Identification and functional characterization of CbaR, a MarR-Like modulator of the cbaABC-encoded chlorobenzoate catabolism pathway. Appl Environ Microbiol 67:3530–3541

Reinecke DM, Bandurski RS (1981) Metabolic Conversion of C-14-Labeled Indole-3-Acetic-Acid to C-14-Labeled Oxindole-3-Acetic Acid. Biochem Bioph Res Co 103:429–433

Sambrook J, Maniatis T, Fritsch EF (1989) Molecular cloning: a laboratory manual. Cold Spring Harbor, N.Y.: Cold Spring Harbor Laboratory. 3 v. p

Spaepen S, Vanderleyden J, Remans R (2007) Indole-3-acetic acid in microbial and microorganism-plant signaling. FEMS Microbiol Rev 31:425–448

Stein SE (1999) An integrated method for spectrum extraction and compound identification from gas chromatography/mass spectrometry data. J Am Soc Mass Spectr 10:770–781